

# **The Automation of Uncrewed Aircraft Systems Traffic Management Calibration Based on Experimental Platform Data**

*Thomas C. Henderson<sup>1</sup>, David Sacharny<sup>1</sup>, Chad  
Mello<sup>2</sup>, and William Raley<sup>1</sup>*

1

UUCS-24-009

## ***Abstract***

Many countries are developing an Urban Air Mobility (UAM) capability defining an Uncrewed Aircraft Systems (UAS) Traffic Management (UTM) architecture to allow safe UAS services in urban environments (e.g., delivery, inspection, air taxis, etc.). The main considerations are air worthiness, operator certification, air traffic management, C2 Link, detect and avoid (DAA), safety management, and security. In addition, if thousands of simultaneous UAS flights are to be achieved, it is not possible for them to be controlled individually by human operators. This makes it necessary to have a rigorous and safe automation methodology to handle such a number of flights. A lane-based airspace structure has been proposed which reduces the complexity of strategic deconfliction by providing UAS agents with a set of pre-defined airway corridors called lanes [14, 15]. This yields collateral benefits including UAS information privacy, robust contingency handling exploiting the lane structure, as well as improved observability and control of the air space. A robust set of UTM parameters and policies must be determined based on the performance characteristics of the deployed UAS platforms, and a methodology which constitutes a first step toward this end is proposed and demonstrated here. In order to realize this approach, a set of initial experiments have been performed to determine the constraints imposed by the UTM on UAS platform capabilities and vice versa. Initial implementation parameters and policies are defined. The major contribution here is a methodology to calibrate UTM safety parameters (e.g., headway, platform speed) in terms of specific platform models' operational characteristics. That is, UTM parameters are a function of platform and not some arbitrarily imposed values. Safety uncertainty is then characterized by the calibration method.

---

<sup>1</sup>1: University of Utah, SLC, UT; 2: US Air Force Academy, Colorado Springs, CO.

# 1 Introduction

Version 1.0 of the Unmanned Aircraft Systems Traffic Management Concept of Operations [4] provides the initial overview of low-altitude UAS operations management from NASA, the FAA and industry partners based on "use-case development, insights on rulemaking, and the evolution of UTM Technical Capability Levels." Figure 1 shows their proposed UTM architecture. This approach requires strategic deconfliction for every flight (i.e., ensure that no two flights get too close), and this is achieved through pairwise 4-D flight path deconfliction. This method suffers from high computational complexity and also requires users to share their flight details with each other in order to perform deconfliction, thus raising privacy concerns.

SESAR JU (the Single European Sky ATM Research, Joint Undertaking) has similarly defined four phases of increasing automation for UAM development, each with increasing automation with the ultimate goal of minimal human interaction [1]. More concrete UTM development has been described by, e.g., Airmap [1], where they describe five essential UTM components: Registry Engine, Geo-Engine, Flight Engine, Traffic Engine, and User Interfaces.

All such approaches have one major thing in common: a safe separation distance between platforms must be determined. This is generally assumed to be a single value selected by the UTM operators. However, we argue here that each UAS platform model should have its own specific headway distance defined in terms of the platform's operational characteristics. This custom headway must be enforced for this particular platform type.

NASA has provided frameworks which motivate our work here. First, the SAFE50

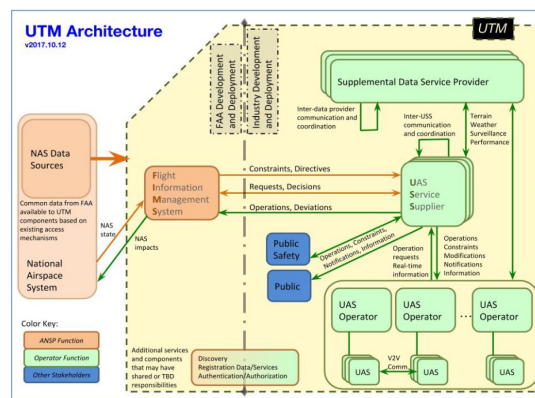


Figure 1: FAA-NASA Proposed UTM Architecture (from [4]).

Reference Design Study "seeks to establish, analyze, and validate an end-to-end reference design for fully autonomous large-scale UAS operations in order to establish a consistent design and complete vertical solution from high-level traffic management down to vehicle sub-system level requirements" [7]. They propose that verification and validation take place not only through simulation studies but also by flight testing hardware prototypes. They state that "there is a lack of validated concept studies, architectures, rules, and requirements in this regime, particularly that address the full design solution from the higher level air traffic management level down to the vehicle sub-system level in a formal, methodical, and traceable manner." In the methodology we propose below, we use their Concept of Operations framework for UTM parameter calibration. In a related work [16], NASA provides a sensitivity analysis of key factors in large-scale UTM operations. They address issues related to vehicle varieties, large-scale operations, the urban environment, and weather. Critical factors studied include communication latency, position accuracy, wind, separation headway and traffic density. This analysis is used to quantify key factor relationships and help determine requisite UTM parameter values to achieve desired safety levels. They call for investigation of route structure based operations taking into account a mix of vehicle types with differing performance characteristics. **This UTM calibration problem is addressed in this work.**

We have previously proposed an alternative lane-based UTM approach which provides many advantages: (1)  $\mathcal{O}(n^2)$  strategic deconfliction complexity, (2) flight information privacy, (3) lane-based contingency handling, (4) network traffic performance measures, and (5) low-complexity flight monitoring and anomaly detection (see [6, 8, 9, 12, 10, 11, 13, 14, 15]). In 2023, the FAA-NASA UAM ConOps Version 2.0 was released [5], and it set the stage for future UTM development through (quoted from [5]):

1. "Initial UTM operations are conducted using new aircraft types that have been certified to fly within the current regulatory and operational environment.
2. A higher frequency (i.e., tempo) of UAM operations in the future is supported through regulatory evolution and UAM Corridors that leverage collaborative technologies and techniques.
3. New operational rules and infrastructure facilitate highly automated cooperative flow management in defined Cooperative Areas (CAs) enabling remotely piloted and autonomous aircraft to safely operate at increased operational tempos."

The FAA and NASA have been moving closer to our lane-based approach (called UAM Corridors by FAA-NASA). Here we aim to advance UAM development by

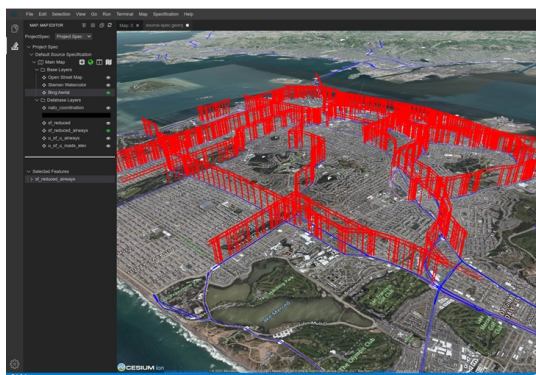


Figure 2: A Small Lane Network over San Francisco, CA.

(1) helping delineate what the platform certification should include in the way of performance requirements as related to specific UTM parameters and policies in order to ensure safe and cooperative operation in dense UAS conditions, and (2) determining how to calibrate UTM parameters and policies to the performance characteristics of particular platforms.

## 2 Background

The lane-based UTM approach has three main components: (1) lane network specification, (2) flight reservation and strategic deconfliction, and (3) UTM operations. Each in turn is briefly described here; for more detailed information see [14, 15].

### 2.1 Lane Specification

A UTM is designed for a specific geographic location and purpose. Figure 2 shows a small network over a part of San Francisco. In general, the network will be developed by a team of UAM stakeholders: urban planners, commercial interests, UAM authorities, etc. In the case shown here, the lanes correspond to the road network on the ground with the addition of launch and land lanes.

This lane network was designed within the GeoRq system which loads designated GIS road network data, and then follows user specifications in terms of lane altitudes, etc. to create what is basically a directed graph; nodes are intersections

between lanes and directed edges are the one-way lanes of the network. The user may specify other types of networks, e.g., grids or Delaunay networks, as deemed necessary.

Once the network is created, it is possible to run network analysis tools to determine bottlenecks, turning angle issues, etc. An iterative design process is continued until a satisfactory result is achieved.

## 2.2 Flight Reservations and Strategic Deconfliction

The details of this aspect are covered in [14, 15], and only a cursory overview is given here. When all UAS speeds are the same, the Lane-Based Strategic Deconfliction (LBSD) algorithm can be used. A flight is defined as a sequence of lanes to traverse in order, starting with a launch lane and ending with a landing lane, where the end of one lane connects to the start of the next. Given such a lane sequence, the strategic deconfliction algorithm seeks a launch time that allows traversal of each lane in the sequence without getting too close to other flights. This is handled using a Space-Time Lane Diagram (STLD) for each lane (much like in standard ground road network analysis); the abscissa is time and the ordinate is distance. Thus, the angle across the diagram indicates the speed. STLDs allow a low complexity algorithm to determine a deconflicted trajectory.

In order to obtain a reservation, a user provides the lane sequence and a possible launch time interval. Only the reservation system is privy to this information and can determine if there is a time to launch that is deconflicted. If there is, then this flight is entered into the system and used to deconflict further future flight requests. Figure 3 shows a flight path (in red) through a simple grid network.

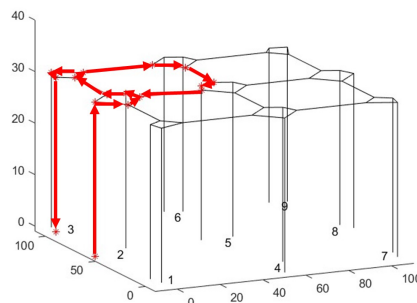


Figure 3: Flight Path (in red) through a Small Grid Network.

## 2.3 UTM Operations: Parameters and Policies

The operational aspects of a UTM are crucial and have been the focus of much current research and indeed a major target of the UAM ConOps Version 2 report. Most of our work to date has been algorithm development or demonstration of the lane-based approach through simulation. We now turn to an investigation of the essential parameters that must be determined for a safe and robust physical realization of a UTM.

### 2.3.1 Basic Requirements for Lane Network Flight

There are some basic requirements for safe and robust large-scale lane network flights. These include:

- Flights must all be strategically deconflicted.
- Flights must maintain their assigned speed in each lane.
- Flights must stay on the lane segments in 3D space.
- Flights must have reliable and timely communications. This is necessary to transmit telemetry data at the required rate as well as to receive UTM instructions.
- Flights must have an emergency landing path at every point in the flight.

Of course, these requirements cannot in general be met with no error. This means that each must have some allowed amount of associated uncertainty. In this case, UTM parameters and policies must be chosen so as to ensure safety even in the face of this uncertainty. We consider each of the above basic requirements in turn. Strategic deconfliction poses less uncertainty than the others since it is a computational problem and involves issues of numerical computation (roundoff, etc.); generally speaking, these are not significant at the scale of operation of physical UAS.

On the other hand, the other basic requirements do involve deviations which risk violating separation constraints. Speed may vary due to fluctuations in power, weather conditions (e.g., wind, rain, etc.), controllers for motors, and sensor error (e.g., ground speed estimates). Errors in following the lane segment may arise due

to GPS problems, weather, lane curvature or lane connection angles, etc. Communication systems require adequate power and available bandwidth; moreover, network and physical security are paramount. Finally, if a UAS is impaired, then it should be able to follow a special emergency landing lane to a pre-specified site; however, in the worst case (e.g., parachute deployment) it may be necessary to land by going straight down to the ground.

### **3 Methodology for Uncertainty Characterization**

To address the issues involving uncertainty which may impact safety distance separation, we consider only aleatoric uncertainty, i.e., the randomness associated with the physical nature of flight. Epistemic uncertainty exists in UAS systems, but is very difficult to identify due to the interaction of algorithmic decision making, physical PID controller impact, and sensor uncertainties. The proposed methodology for uncertainty characterization is:

1. Identify the variables whose uncertainty is to be quantified.
2. Develop a set of flight scenarios which permit observations of these variables to be gathered.
3. Run a set of experiments, gather the data, and use the mean and variance to characterize the uncertainty.

Once the uncertainty has been quantified in this way for a specific platform, it is possible to choose UTM parameter values so as to keep the risk of violating the constraint below a specified probability.

We choose the NASA Concept of Operations framework [7] as the basis for our work. The primary use case is point-to-point (e.g., like package delivery) which assumes:

- reliable UAS to ground communications
- the mission objective is provided to the UAS onboard autonomy subsystem by the UAS operator
- operational volumes are produced around the planned trajectory
- human interaction is allowed

- the UAS flight plan must be strategically deconflicted
- the UAS must meet minimum performance requirements.

Our view is that a UTM should accommodate as wide a selection of UAS platform types as possible. To that end, a UAS manufacturer will present *calibration* data which characterizes the ability of the platform to stay in the lane center and maintain the prescribed speed (along the lane). This allows less reliable platforms to fly, but will impose larger separation headway (perhaps making it more difficult for them to schedule a flight during high-density operations).

## 4 Experiments

Two platforms have been calibrated using this approach: (1) the Tarot X6-based hexacopter platform from UAV Systems International [2] in an outdoor setting. These have highly disparate performance characteristics, and (2) the Crazyflie platform [3] in an indoor setting. The experimental protocol is as follows:

- A lane network is created using the SkyLanes system.
- A flight mission is specified; i.e., a sequence of lanes through the lane network and a speed in each lane.
- The flight reservation systems approves the flight and adds it to the UTM system.
- The lane endpoints are used as waypoints and provided for loading into the UAS mission execution system. Note that for the outdoor UAV tests this involved GPS waypoints, while for the indoor tests this was a set of  $x, y, z$  endpoint values.
- The missions were flown and telemetry data from the UAVs used to determine the safety parameter values.

### 4.1 X6 Hexacopters

Each hexacopter has an Intel RealSense D455 depth-sensing camera (although they are not used in these experiments), the PX4 (ArduPilot) Cube Blue autopilot,



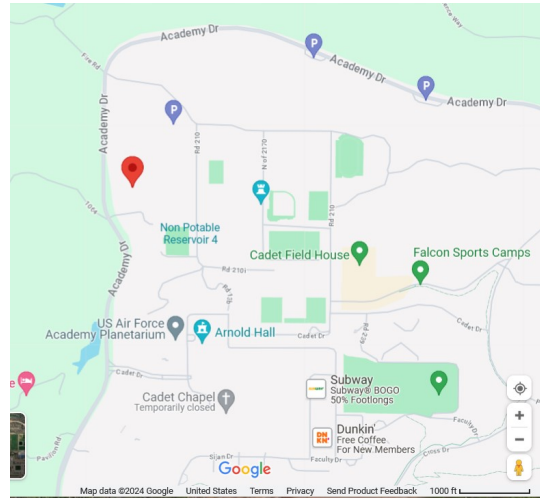


Figure 4: Map of Experiment 1 Location on Air Force Academy Grounds.



Figure 5: Picture of Experiment Location with Grid Corners Indicated.

the NVIDIA Jetson Xavier NX for accelerated AI execution – 6-core ARM CPU, 384 GPU cores, 8 GB ram, and 1TB SSD. In terms of software, all programming is done in Python using the PyCharm development environment; this is a free, open-source, robust system that provides virtual environment creation, debugging and syntax checking. Two drone-related API libraries are used: Pymavlink and DroneKit. Communication with the drone takes place using serial communication using the MavLink protocol. Mission Planner is used to configure the drone hardware, upload flight plans, and monitor drones while in flight.

The test flight location is on the Air Force Academy grounds; Figure 4 shows a map of the location (marked with red balloon), while Figure 5 shows a picture of the site with the corners of the grid lane network indicated by the red dots.

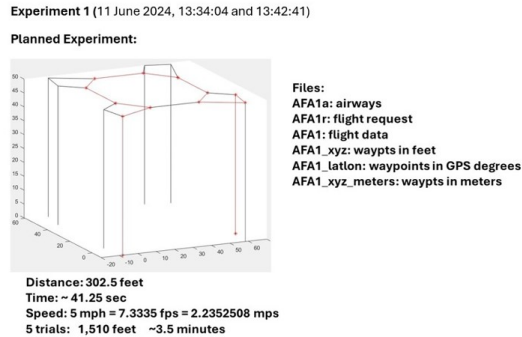


Figure 6: Lane Network and Simple First UAS Route.

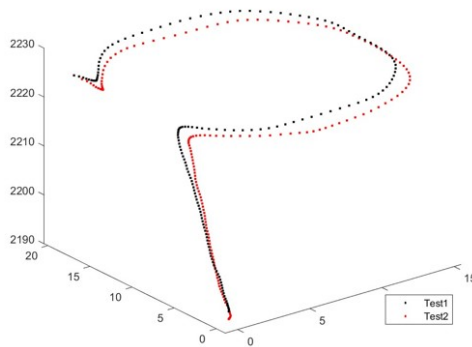


Figure 7: Telemetry Data for Two Flights of Simple First UAS Route.

#### 4.1.1 Single UAS: First Simple Route

In order to debug the UTM calibration process, a first experiment was run on a simple up, over and down route. Figure 6 shows the lane network and route. Two flights were run and their trajectories are shown in Figure 7. Figure 8 shows the speeds during the two flights, and as can be seen, once at the upper level of the lane network, the average speed was near the commanded speed of 2.5 meters per second. Figure 9 shows the telemetry data overlayed on the lane network. Figure 10 shows Prof. Mello at the test site, Figure 11 shows Prof. Mello preparing the hexacopter for launch, and Figure 12 shows Prof. Mello preparing the mission control interface.

Figure 13 shows the hexacopter at the launch position; Figure 14 shows the flight just after takeoff, and Figure 15 shows mid-flight.

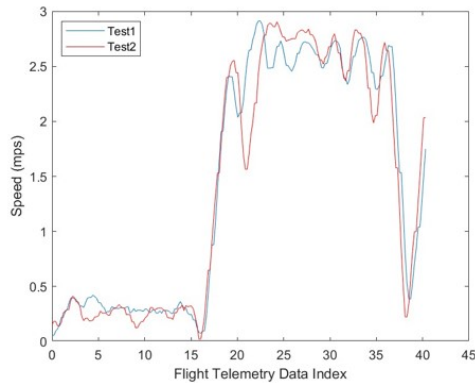


Figure 8: Speeds for Two Flights of Simple First UAS Route.

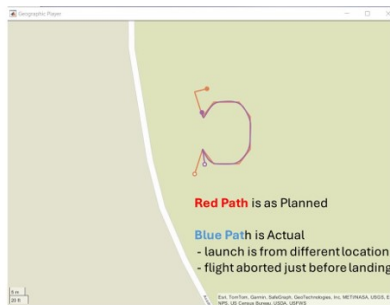


Figure 9: Telemetry Data for Two Flights of Simple First UAS Route Overlaid on Lane Network.

#### 4.1.2 Single UAS: More Complex Flight Path

The planned flight path is shown in Figure 16. The major goal was to create a network, plan a path through its lanes, and determine repeatability. The flight begins in the lower left corner, goes north, makes the small loop in the upper left corner, then makes the (clockwise) outer loop to land at the launch point.

These tests were flown on 25 June 2024 with the temperature of 89 degrees and the wind between 5-8 mph. Figure 17 shows the drone at takeoff and in flight.

Five flights were flown to obtain the data necessary to calibrate the UTM safe headway parameter. Figure 18 shows the flight telemetry data from one flight as a 3D overlay on the lane network, while Figure 19 shows a projection onto the ground plane.

The mission tracker screen is shown in Figure 20 with the left side at the start of the flight, and the right side in the first interior loop. Finally, the distance from lane



Figure 10: Prof. Mello at UAS Test Site.

statistics gathered from the flight are shown in Figure 21. The safety headway distance is established by running  $n = 5$  experiments, and finding the mean distance from the lane for each. The mean,  $\mu$ , and (sample) variance  $S^2(n)$ , are found; finally, a confidence interval is found for the error and a safety headway distance is at least double that (since the two aircraft errors add). For example, the 99 percent confidence interval is:

$$\mu \pm 3.747 \sqrt{\frac{S^2(n)}{n}}$$

Thus, the large end error of this confidence interval for  $\mu = 1.5409$  feet and  $S^2(5) = 0.0025$  is 1.6247 feet. This should be doubled for the case of two aircraft, indicating that a minimum of 3.2493 feet suffices for 99 percent confidence. In this case a UTM administrator could choose from 4 to 6 feet to further increase the safety margin.

More information was gathered for these flights, and data from the first flight includes the distance from the intended lane shown in Figure 22, error in heading in Figure 23, and nearest lane index shown in Figure 24. The error analysis is given above over all tests; the error in heading spikes at the lane turns, but is otherwise reasonable, and the nearest lanes are all correct indicating good robustness of the system.



Figure 11: Prof. Mello preparing Hexacopter for Launch.

#### 4.1.3 Two UAS Test

Based on the calibration information from the single UAS test flights, a two UAS test was created. Figure 25 shows the route for the first flight while Figure 26 shows the path for the second flight. Figure 27 shows the two UAS at their launch positions. Finally, Figure 28 shows the telemetry data from the two platforms during a test run. As can be seen, the paths share a common lane, and the deconfliction algorithm separates them according to the desired headway, and the result is a safe airway.

#### 4.2 Crazyflies

The Crazyflie 2.1 is a small flying development platform that weighs 27g and has about a 3" radius. It is equipped with low-latency/long-range radio as well as Bluetooth LE. The system can be flown from iOS and Android with Bluetooth LE, as well as from Windows/Mac OSX/Linux with the Crazyradio. The Dual-MCU architecture has dedicated radio/power management SoC for advanced applications. Also included is real-time logging, graphing and variable setting in addition to full use of expansion decks. The onboard microcontrollers include the STM32F405 main application MCU (Cortex-M4, 168MHz, 192kb SRAM, 1Mb flash), nRF51822 radio and power management MCU (Cortex-M0, 32Mhz, 16kb SRAM, 128kb flash) and a micro-USB connector along with an 8KB EEPROM. Sensors include a 3 axis ac-



Figure 12: Prof. Mello preparing Mission Control Interface.



Figure 13: UAS Ready for Launch.

celerometer/gyroscope (BMI088) and a high precision pressure sensor (BMP388). There is a 2.4GHz ISM band radio with increased range with 20 dBm radio amplifier and dual antenna support with both on board chip antenna and U.FL connector. Finally, flight time with stock battery is 7 minutes, and the maximum recommended payload weight is 15 g. (This information is paraphrased from [3].)

A major issue for the Crazyflie is the localization method:

The Loco Positioning system is a local positioning system, based on Ultra Wide Band radio that is used to find the absolute 3D position of objects in space. It is in many ways similar to a miniature GPS system.

The base of the system is a set of Anchors that are positioned in the



Figure 14: UAS just after Takeoff.



Figure 15: UAS Mid-flight.

room (compare to the satellites in GPS), they are the reference. The other part of the system is one or more Tags (compare to the GPS receiver) that are fixed to the object(s) that are to be tracked. By sending short high frequency radio messages between the Anchors and Tags, the system measures the distance from each Anchor to the Tags and calculates the position of the Tags from that information.

All information needed to calculate the position is available in the Tag which enables position estimation on board the Crazyflie, as opposed to many other positioning systems where the position is calculated in an external computer and sent to the Crazyflie.

By adding knowledge of its position to a Crazyflie 2.X, it is capable of flying autonomously without manual control. This opens up an array of exciting use cases and applications.

What this means in terms of the experiments is that the localization is not very precise and error depends on the X-Y-Z position in the indoor space due to the interference of furniture and other objects in the room. This gives us an example of very poor conditions to see how the calibration method responds. The test flight is

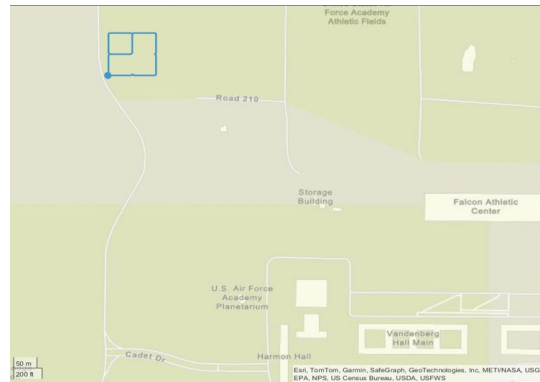


Figure 16: Planned Simple Route for Single UAS Flight.



Figure 17: Telemetry Data for Single UAS Flight.

an indoor location enclosed by a netting frame. The overlay of the flight telemetry data from one flight and the lanes network is shown in Figure 29. The major goal was to have motions through all coordinate dimensions and determine repeatability. Figure 30 shows a Crazyflie in flight. Ten flights were flown to obtain the data necessary to calibrate UTM safety headway. The distance from lane statistics are shown in Figure 31.

The other ten flights are shown in Figures 32- 40.

Here there are 10 experiments and the mean distance error is 0.7372 feet and  $S^2(10) = 0.00011$ , so the large end error of the confidence interval is  $0.7372 + 2.821 * \sqrt{0.00011/10} = 0.7684$  feet headway. When doubled this yields a minimum safety headway distance of 1.5368 feet.

## 5 Conclusions and Future Work

In order to realize safe, robust implementations of large-scale UAS operations, it is necessary to determine the parameters of the UTM. One such method is proposed here along with some first experiments to validate this approach on two distinct



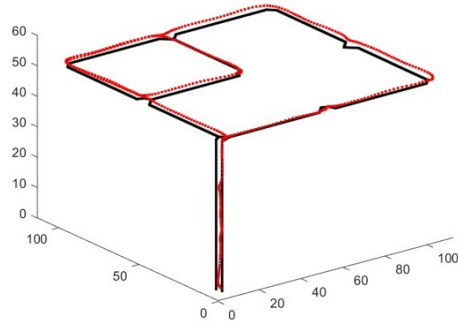


Figure 18: 3-D Overlay of Flight Telemetry Data with Lane Network.

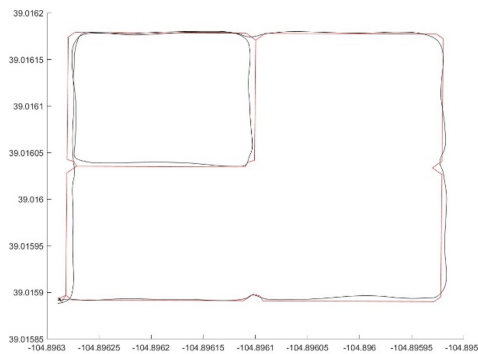


Figure 19: Ground Projection Overlay of Flight Telemetry Data with Lane Network.

types of platforms. In order to achieve this validation, a lane network is created, the flight lane sequences are scheduled using the lane-based strategic deconfliction method, and the first lane-based flights were flown both outdoors and indoors.

Future work includes:

- further validation tests in larger testbed settings,
- calibration which takes into weather into account (e.g., wind, rain, snow, humidity, etc.),
- validation of multiple simultaneous UAS flights over long time periods,
- dynamic lane creation for contingencies, including emergency landings.

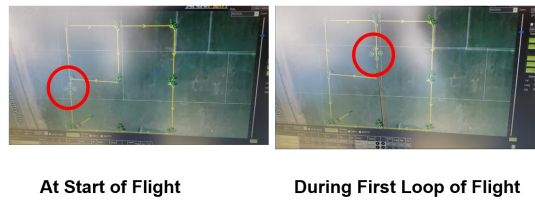


Figure 20: Mission Tracking Interface View During Flight.

(Error in Feet)	Mean Error	Max Error	Min Error	Error Variance
1	1.5678	3.3971	0.2253	0.6068
2	1.5579	3.5935	0.0647	0.9027
3	1.6006	3.5301	0.4545	0.5523
4	1.4844	3.3744	0.0711	0.6095
5	1.4937	3.4823	0.1233	0.6361
<b>Mean Values:</b>	<b>1.5409</b>	<b>3.4755</b>	<b>0.1878</b>	<b>0.6615</b>

Figure 21: Single UAS Simple Path Lane Distance statistics.

## ACKNOWLEDGMENT

This work was supported in part by an Air Force Summer Faculty Fellowship.

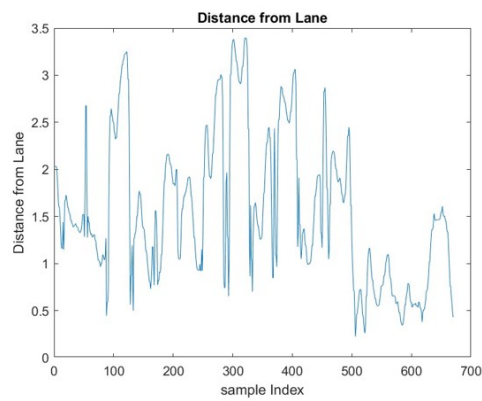


Figure 22: Distance from Lane during Flight.

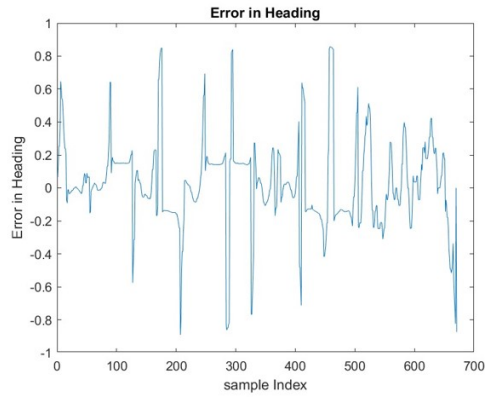


Figure 23: Error in UAS Heading during Flight.

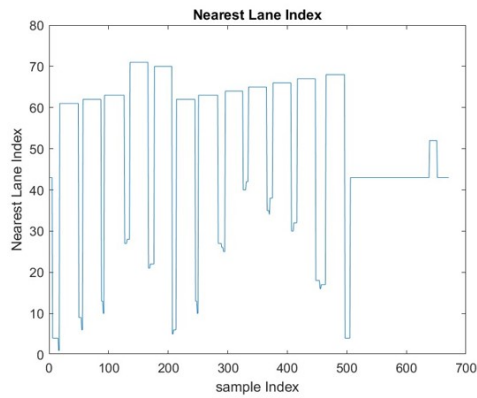


Figure 24: Nearest Lane Index during Flight.

## References

- [1] Airmap. Five Critical Enablers for Safe, Efficient and Viable UAS Traffic Management (UTM), January 2018.
- [2] [uavsystemsinternational.com](http://uavsystemsinternational.com).
- [3] [www.bitcraze.io](http://www.bitcraze.io).
- [4] Steve Bradford. *Unmanned Aircraft Systems Traffic Management Concept of Operations, Version 1.0*. US Department of Transportation, Federal Aviation Administration, Washington, DC, May 2018.
- [5] Paul Fontaine. *Urban Air Mobility Concept of Operations, Version 2.0*. US Department of Transportation, Federal Aviation Administration, Washington, DC, April 2023.

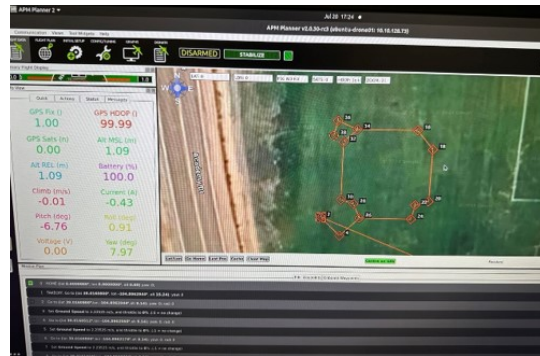


Figure 25: First UAS Route for Two Flight Test.



Figure 26: Second UAS Route for Two Flight Test.

- [6] T C Henderson, D Sacharny, and M Cline. An Efficient Strategic Deconfliction Algorithm for Lane-Based Large-Scale UAV Flight Planning. Technical Report UUCS-19-005, University of Utah, September 2019.
- [7] C.A. Ippolito, K. Krishnakumar, V. Stepanyan, A. Chakrabarty, and J. Bacali. SAFE50 Reference Design Study for Large-Scale High-Density Low-Altitude UAS Operations. In *IAA SciTech Forum*, San Diego, CA, January 2019.
- [8] D. Sacharny and T.C. Henderson. A Lane-Based Approach for Large-Scale Strategic Conflict Management for UAS Service Suppliers. In *2019 International Conference on Unmanned Aircraft Systems (ICUAS)*, pages 937–945, Atlanta, GA, June 2019. Institute of Electrical and Electronics Engineers (IEEE).
- [9] D. Sacharny and T.C. Henderson. Optimal Policies in Complex Large-scale UAS Traffic Management. In *IEEE International Conference on Industrial Cyber-Physical Systems*, Taipei, Taiwan, May 2019.



Figure 27: Two UAS at Launch Locations for Two Flight Test.

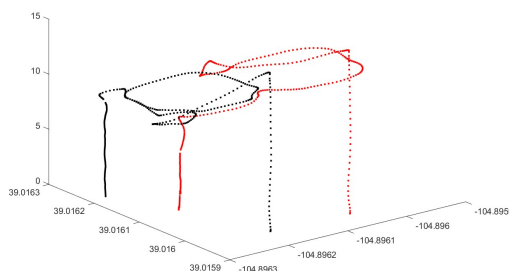


Figure 28: Telemetry Data for Two Flights during Two Flight Test..

- [10] D. Sacharny, T.C. Henderson, and M. Cline. Large-Scale UAS Traffic Management (UTM) structure. In *IEEE Multisensor Fusion and Integration Conference*, Karlsruhe, Germany, September 2020.
- [11] D. Sacharny, T.C. Henderson, M. Cline, B. Russon, and E. Guo. FAA-NASA vs. Lane-Based Strategic Deconfliction. In *IEEE Multisensor Fusion and Integration Conference*, Karlsruhe, Germany, September 2020.
- [12] D. Sacharny, T.C. Henderson, and E. Guo. A DDDAS Protocol for Real-Time UAS Flight Coordination. In *InfoSymbiotics/Dynamic Data Driven Applications Systems Conference*, Boston, MA, October 2020.
- [13] D. Sacharny and C. Liu. Strategic Deployment of Drone Centers and Fleet Size Planning for Drone Delivery, Report No. UT-21.33. Technical report, Utah Department of Transportation, Salt Lake City, UT, 2021.
- [14] David Sacharny and Thomas C. Henderson. *Lane-Based Unmanned Aircraft Systems Traffic Management*. Springer, New York, NY, 2022.

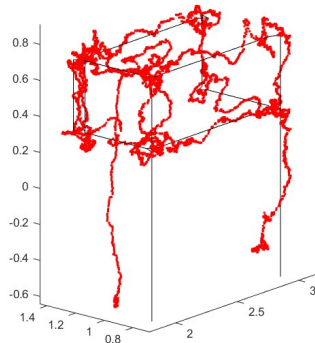


Figure 29: Overlay of Crazyflie Flight Telemetry Data with Lane Network.

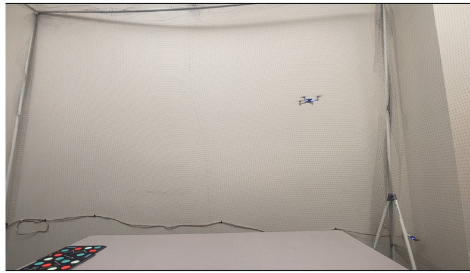


Figure 30: Crazyflie in Flight in Cage.

- [15] David Sacharny, Thomas C. Henderson, and Vista Marston. Lane-Based Large-Scale UAS Traffic Management. *Transactions on Intelligent Transportation Systems*, 23(10):18835–18844, 2022.
- [16] M. Xue. Sensitivity Analysis of Ky Factors in High Density Unmanned Aerial System Operations. In *IAA SciTech Forum*, San Diego, CA, January 2019.

Flight Number	Mean	Max	Min	Error
	Error	Error	Error	Variance
1.0000	0.2227	0.7867	0.0003	0.0218
2.0000	0.2293	0.9171	0.0020	0.0267
3.0000	0.2277	0.8324	0.0014	0.0270
4.0000	0.2448	1.0467	0.0003	0.0428
5.0000	0.2316	0.9766	0.0005	0.0336
6.0000	0.2315	0.8502	0.0021	0.0258
7.0000	0.2215	0.8786	0.0002	0.0228
8.0000	0.2071	0.7303	0.0023	0.0183
9.0000	0.2141	0.8745	0.0023	0.0239
10.0000	0.2170	0.9662	0.0004	0.0375

Mean Values (m): 0.2247 0.8859 0.0012 0.0280

Figure 31: Crazyflie Flight Error Statistics over Ten Test Flights.

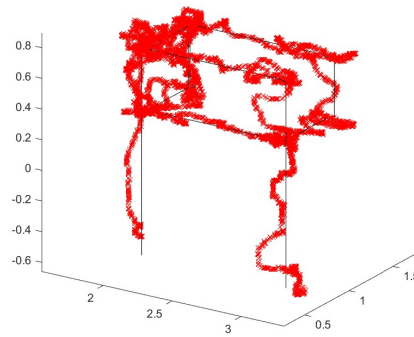


Figure 32: Crazyflie Flight 2.

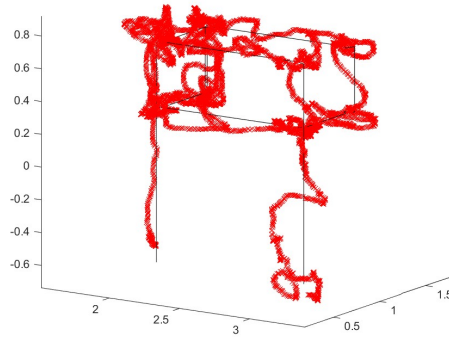


Figure 33: Crazyflie Flight 3.

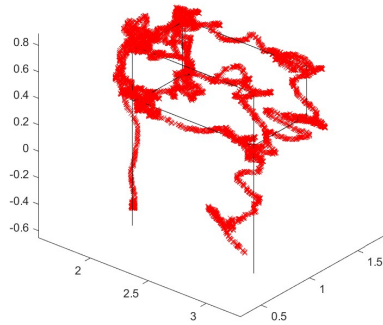


Figure 34: Crazyflie Flight 4.

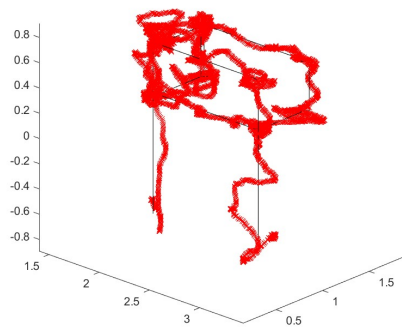


Figure 35: Crazyflie Flight 5.



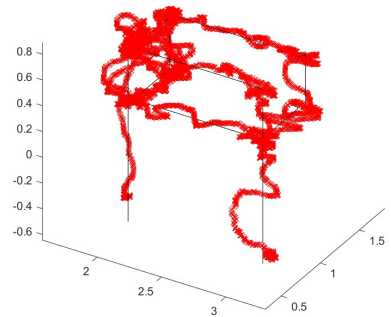


Figure 36: Crazyflie Flight 6.

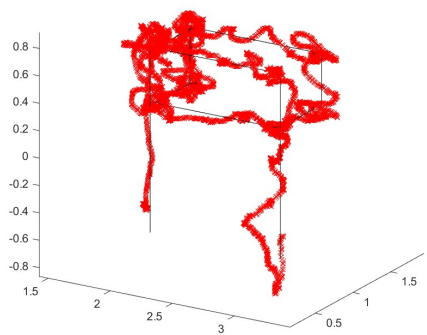


Figure 37: Crazyflie Flight 7.

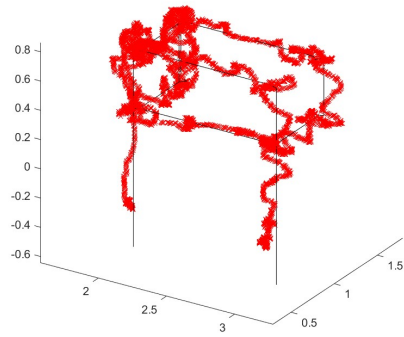


Figure 38: Crazyflie Flight 8.

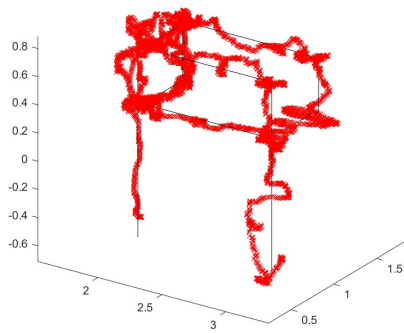


Figure 39: Crazyflie Flight 9.

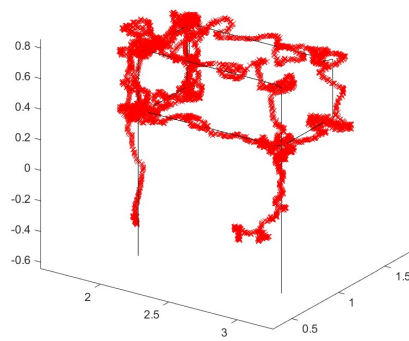


Figure 40: Crazyflie Flight 10.